https://doi.org/10.5194/egusphere-2026-2913
Preprint. Discussion started: 6 August 2026

Development and application of a physics-constrained adaptive decomposition model for displacement sequences of step-like landslide

Yimin Liu[1], Yixuan Li[3], Xiaoliang Feng[2], Huan Chen[2*]

[1]College of Artificial Intelligence, Chengdu Technological University, Chengdu, 611730, China
[2]China Geological survey Institute of Exploration Technology, Chinese Academy of Geological Sciences, Chengdu, 611734, China
[3]Graduate School of Advanced Science and Technology, Japan Advanced Institute of Science and Technology, Nomi, Ishikawa, 923-1292, Japan

Correspondence to: Huan Chen (chuan@mail.cgs.gov.cn)

Abstract. Addressing the nonlinear evolution of step-like landslides in China's Three Gorges Reservoir area, which is driven by the strong coupling of reservoir water level fluctuations and rainfall pulses, this paper proposes a highly adaptive and physics-constrained displacement decomposition framework. First, a Chebyshev-Lévy flight-enhanced sparrow search algorithm (CLF-SSA) is developed to adaptively optimize the core parameters of variational mode decomposition (VMD). Concurrently, an integrated objective function — incorporating mathematical sparsity (envelope entropy) and a physical correlation penalty for the periodic component—is constructed. This framework ensures that the decomposition process is mechanistically-driven from its foundational level, maintaining a strictly physics-constrained architecture. Secondly, a multi-dimensional quantitative reconstruction strategy for intrinsic mode functions (IMFs) is established, integrating central frequencies, correlations with multi-source environmental factors (reservoir water level, rainfall, and elevation), and seasonal energy distribution. This strategy enables the robust decoupling of cumulative displacement sequences into distinct trend, periodic, and random components, effectively mitigating the phenomenon of mode mixing. Finally, the surface displacement of a representative step-like landslide in the TGR area was decomposed using the proposed framework. The results demonstrate that the model achieves sub-millimeter reconstruction precision, with an average root mean square error (RMSE) of approximately 0.5 mm. Notably, the decoupled periodic components exhibit exceptional consistency with geomechanical responses, achieving a maximum correlation gain of 4283.60%. By incorporating the PyLith continuous-slip numerical model for physical validation, this study effectively elucidates the displacement step-triggering mechanism induced by seepage pressure during reservoir drawdown. This transition from statistical identification to mechanistic interpretation provides robust physical support for overcoming the pervasive time-lag bottlenecks in landslide early warning engineering. Future research will focus on integrating this physics-constrained decomposition framework with deep learning models to enhance the real-time predictive capability for diverse landslide types.

https://doi.org/10.5194/egusphere-2026-2913
Preprint. Discussion started: 6 August 2026

1 Introduction

As a unique and highly challenging hazard type in the Three Gorges Reservoir (TGR) area of China, the evolution of step-like reservoir landslides is profoundly driven by the strong coupling of dynamic environmental factors, particularly periodic reservoir water level fluctuations and intensive rainfall (Guo et.al, 2022). The cumulative displacement curves of these landslides exhibit a distinctly non-stationary "step-like" pattern, characterized by impulsive acceleration triggered under specific hydrological conditions, followed by periods of relatively stable creep. Such highly nonlinear dynamic evolutionary characteristics make these landslides a natural laboratory for elucidating "water-soil-dynamics" coupling failure mechanisms. However, their complex time-frequency attributes during the evolutionary process also pose significant technical challenges for precise stability assessment and proactive risk early warning (Yin, 2005).

The water level operation in the TGR area is primarily governed by anthropogenic seasonal regulation, following a recurring pattern of "low water levels for flood control" during the flood season and "high water levels for storage" thereafter, with an annual fluctuation amplitude reaching 30–40 meters (Sun and Zhao, 2019). Due to the inherent heterogeneity of the slope's permeability, the hydraulic head difference generated during reservoir drawdown induces significant outward seepage pressure, which acts as the dominant driving force for triggering displacement steps in landslides (Lu et.al, 2014; Deng et.al, 2020; Feng et.al, 2023). Furthermore, intensive rainfall serves as another critical trigger (Chen et.al, 2005); by infiltrating and recharging the groundwater table, it reduces the effective stress of the slip zone soil. During periods of water level fluctuation, rainfall exerts an "incremental compensation" or "reactivation" effect, synergistically accelerating landslide evolution (Guo et.al, 2020; Li, 2023; Qu et.al, 2025). Consequently, the high-fidelity isolation of environment-driven displacement components from complex raw signals, coupled with the precise capture of their nonlinear mapping relationships with deformation transition points, remains the core challenge in enhancing the accuracy and timeliness of early warning systems.

With the advancement of nonlinear system theory and machine learning, time-series decoupling has emerged as a mainstream approach for enhancing the interpretability of landslide deformation evolution, progressively superseding traditional empirical analyses and statistical methods (Chae et.al, 2017; Segoni et.al, 2018). Recent studies have extensively introduced techniques such as Holt’s double exponential smoothing (Pardeshi et.al, 2013), empirical mode decomposition (EMD) (Meng et.al, 2023) and its derivatives (e.g., EEMD) (Wang et.al, 2023), as well as variational mode decomposition (VMD), which possesses a robust variational theoretical foundation (Dragomiretskiy and Zosso, 2013; Guo et.al, 2020). Furthermore, research has explored hybrid models optimized by swarm intelligence algorithms (Jiang et.al, 2022; Ren et.al, 2025) and singular spectrum analysis (SSA) (Xiang et.al, 2025). The core logic of these methodologies lies in decomposing complex cumulative displacement sequences into geological-baseline-driven trend components and hydrological-trigger-driven fluctuating components (comprising periodic and random terms). This aims to quantitatively characterize the nonlinear mapping relationships and response lag features between reservoir water levels, rainfall, and slope response.

https://doi.org/10.5194/egusphere-2026-2913
Preprint. Discussion started: 6 August 2026

Table 1 Summary of Llandslide deformation decomposition methods

Methods	Characteristics	Disadvantage
Holt's double exponential smoothing	Improve the fitting effect of trend displacement by uneven weighting	Limit adaptability to abrupt changes
Empirical mode decomposition (EMD)	Adapt to the data changing characteristics and improve the decomposition accuracy	Modal aliasing when dealing with sudden signal change
Ensemble empirical mode decomposition (EEMD)	Enhances scale adaptability of the signal and makes boundary of the Intrinsic Mode Function (IMF) component clearer	Computationally expensive and sensitive to the parameter selection
Variational mode decomposition (VMD)	The distinct frequency characteristics mitigating mode mixing and improving decomposition reliability	Over-reliance on parameter selection leads to inefficiency and reduced interpretability
VMD with [article swarm optimization (PSO)	Automatically optimize the key parameter and improve the generalization ability	Premature convergence and suboptimal parameter tuning
VMD with CLF-SSA	Improve the decomposition accuracy and the physical interpretability by optimizing VMD parameters	Classification logic is insufficiently detailed and the dimensions are monotonous
Singular spectrum analysis	Non-parametric, decomposes nonlinear time series with robust denoising	Suffers from subjective L tuning and poor step-like mutation separation

As summarized in Tab. 1, although methodologies ranging from traditional smoothing techniques to advanced Variational Mode Decomposition (VMD) and its derivatives have been widely applied in landslide research, they still confront several fundamental limitations when processing step-like displacement signals characterized by high abruptness:

First, the mechanistic dissociation in the parameter optimization process. The parameter tuning of traditional algorithms, such as VMD or PSO-VMD, relies heavily on mathematical sparsity metrics like envelope entropy. This purely data-driven logic overlooks the inherent constraints between modal components and geophysical triggers. Consequently, while the resulting components may appear mathematically sound, they often lack explicit physical correspondence or even generate uninterpretable spurious components, also known as pseudo-modes.

Second, the dimensional simplification of modal aggregation criteria. Existing classification logics depend excessively on the single Pearson correlation coefficient (PCC). Amidst complex step-like evolutionary processes, such criteria struggle to distinguish physical fluctuations caused by intricate seepage from purely stochastic monitoring noise. As a result, critical random mutation terms induced by short-term intensive rainfall — which possess significant early warning value — are frequently misidentified as noise and filtered out. This diminishes the model's sensitivity in capturing responses to extreme weather events.

To address the limitations of existing models in terms of physical logic and reconstruction criteria, this paper proposes a highly adaptive and physics-constrained displacement decomposition framework for step-like landslides. By deeply

https://doi.org/10.5194/egusphere-2026-2913
Preprint. Discussion started: 6 August 2026

embedding geophysical mechanisms into data-driven algorithms—utilizing an enhanced intelligent optimization algorithm and an integrated objective function — this study aims to resolve the challenge of mechanistic dissociation in the decomposition of highly nonlinear signals. Furthermore, by incorporating the PyLith continuous-slip numerical model (Aagaard et.al, 2017) for physical validation, a precise alignment between decomposed displacement components and deep geomechanical responses is achieved. This framework not only provides a high-fidelity data foundation for quantitatively elucidating the step-triggering mechanisms induced by seepage pressure during reservoir drawdown but also offers robust theoretical support and numerical evidence for overcoming pervasive time-lag bottlenecks in landslide early warning engineering and enhancing geological hazard risk management.

2 Methodology

2.1 Time series analysis

Driven by the dual influence of the subtropical monsoon climate and the cyclical "winter impoundment and summer drawdown" regulation of the TGR area , reservoir-bank landslides in the region commonly exhibit distinct step-like deformation characteristics. Macroscopically, the displacement-time curves manifest as non-stationary time series with a pronounced long-term growth trend; microscopically, they are characterized by instantaneous acceleration phases triggered by environmental environmental factors (Wen et al., 2017). According to time-series decomposition theory, the cumulative displacement $X(t)$ is conceptualized as a composite process resulting from the superposition of three distinct components: a trend component governed by internal geological conditions, a periodic component driven by external environmental triggers, and a stochastic term excited by abrupt disturbances (Box et al., 2015).

To elucidate the response mechanisms of step-like landslides driven by the combined influence of reservoir water level fluctuations and rainfall, this study formalizes the raw cumulative displacement sequence $X(t)$ using an additive model as follows:

$$X(t)=X_{tre}(t)+X_{per}(t)+X_{ran}(t)+\epsilon \quad (1)$$

Where,

- $X_{tre}(t)$ is the trend component: A monotonically increasing nonlinear process governed by the internal geological structure and long-term creep characteristics of the slope.
- $X_{per}(t)$ is the periodic component: A cyclical component strongly regulated by external seasonal hydrological environments (e.g., periodic fluctuations of reservoir water levels), representing the primary contributor to the step-like deformation characteristics.
- $X_{ran}(t)$ is the random component: A stochastic component excited by abrupt factors such as short-term intensive rainfall, earthquakes, or anthropogenic disturbances, reflecting the non-stationary and impulsive mutation features of the displacement signal.

https://doi.org/10.5194/egusphere-2026-2913
Preprint. Discussion started: 6 August 2026

- ϵ denotes the measurement noise or residual term associated with the monitoring system.

For step-like landslides, the inherent complexity of the displacement signal lies in the fact that the periodic component $X_{per}(t)$ and the random component $X_{ran}(t)$ frequently exhibit non-stationary and overlapping characteristics in the frequency domain. Traditional filtering methods struggle to achieve a perfect separation of physical components while preserving the integrity of "step-jump" edges and effectively eliminating high-frequency noise. Consequently, a decomposition tool with superior time-frequency resolution is required to facilitate the precise isolation of these physical constituents.

2.2 Variational mode decomposition (VMD)

Variational Mode Decomposition (VMD) is an adaptive and quasi-orthogonal signal decomposition methodology that decomposes the raw displacement signal into a series of Intrinsic Mode Functions (IMFs), each characterized by a specific central frequency and bandwidth, by constructing and solving a constrained variational problem (Dragomiretskiy and Zosso, 2014). Compared to Empirical Mode Decomposition (EMD), VMD effectively overcomes the issue of mode mixing and demonstrates superior noise robustness by incorporating a quadratic penalty factor and Lagrange multipliers within its variational framework (Raj and Ray, 2017).

- Construction of the constrained variational model. To minimize the sum of the estimated bandwidths of the demodulated modes, VMD identifies the optimal modal components by constructing the following constrained variational expression, as presented in Eq. (2):

$$\begin{cases} min_{\{u_k\},\{\omega_k\}} \left\{\sum_{k=1}^{K} \left\|\partial_t\left[\left(\delta(t)+\frac{j}{\pi t}\right)*\ u_k(t)\right]e^{-j\omega_k t}\right\|_2^2\right\} \\ \qquad s.t.\ \sum_{k=1}^{K} u_k(t)=f(t) \end{cases} \tag{2}$$

Where u_k represents the k-th modal component; ω_k denotes the corresponding central frequency; and $\delta(t)$ signifies the Dirac delta distribution.

- Optimization of the global solution. By introducing the Lagrange multiplier λ_k and the quadratic penalty factor a, the aforementioned constrained problem is transformed into an unaugmented Lagrangian functional. The modal components and their respective central frequencies are iteratively updated through an alternating direction method of multipliers (ADMM) until the optimal solution is obtained, as formulated in Eq. (3):

$$L(\{u_k\},\{\omega_k\},\lambda)=\alpha\sum_k\left\|\partial_t\left[\left(\delta(t)+\frac{j}{\pi t}\right)*\ u_k(t)\right]e^{-j\omega_k t}\right\|_2^2+\left\|f(t)-\sum_k u_k(t)\right\|_2^2+\langle\lambda(t),f(t)-\sum_k u_k(t)\rangle \tag{3}$$

Despite the inherent advantages of VMD in processing non-stationary sequences, several critical limitations persist when characterizing the nonlinear displacement signals of step-like landslides:

- Non-adaptability of Parameter Preset: The number of modes, k, directly determines the frequency resolution, while the penalty factor, α, dictates the compactness of the frequency bands. Step-like signals exhibit broadband characteristics at

https://doi.org/10.5194/egusphere-2026-2913
Preprint. Discussion started: 6 August 2026

mutation points; inappropriate selection of k or α causes abrupt displacement information to be dispersed across multiple modes, resulting in severe mode mixing.

- Decoupling from Physical Interpretability: The optimization process in Eq. (2) is based purely on mathematical signal purity. Due to the absence of a priori constraints from hydrological driving factors, the decomposed components-while achieving mathematical optimality-frequently fail to establish an accurate physical mapping with the periodic or random terms of the landslide displacement signal.

2.3 Parameter optimization based on CLF-SSA

To eliminate the blindness associated with manual parameter presetting in VMD, this study introduces the Sparrow Search Algorithm (SSA) for adaptive parameter optimization. Building upon the standard SSA and addressing the complexity of nonlinear landslide displacement signals, an enhanced CLF-SSA framework is constructed. This framework incorporates improvements across three dimensions: population diversity, global search capability, and a physics-constrained mechanism.

2.3.1 Population initialization based on Chebyshev map

he standard SSA utilizes stochastic methods for population initialization, which often leads to an uneven distribution of initial solutions within the parameter space. This, in turn, can trigger convergence delays or cause the algorithm to fall into local optima traps (Guo et al., 2020). To enhance population diversity, this study introduces the Chebyshev chaotic map to optimize the initial distribution of k and α. The expression for this mapping is presented in Eq. (4).

$$X_{n+1}=cos(k{\cdot}arccosX_n), \quad X\in[-1, 1] \tag{4}$$

The algorithm maps the parameter space onto the feasible domain of VMD via chaotic sequences, ensuring that the initial search points adequately cover diverse combinations of frequency resolution (governed by k) and bandwidth smoothness (governed by α). This strategy significantly enhances the convergence speed and stability of the optimization process.

2.3.2 Global search enhancement via Lévy flight

Step-like displacements exhibit extreme nonlinearity at mutation transition points, making traditional optimization prone to falling into local extrema. To address this, this study integrates a Lévy flight strategy into the position update mechanism of the sparrow search algorithm. By leveraging the stochastic walking characteristics of Lévy flights — defined by a combination of frequent short-distance jumps and occasional long-distance leaps—the algorithm's capability to escape local traps is significantly enhanced. The improved coordinate iteration formula is presented in Eq. (5).

$$X_{ij}^{t+1}=X_{test}(t)+X_{test}(t)\otimes Levy(e) \tag{5}$$

In Eq. (5), $X_{test}(t)$ denotes the current global optimal position (i.e., the optimal combination of k^* and a^* identified in the current iteration). This mechanism significantly increases the probability of the algorithm escaping local extrema, ensuring

https://doi.org/10.5194/egusphere-2026-2913
Preprint. Discussion started: 6 August 2026

both the efficiency and precision of the optimization process. Through the adaptive synergistic search of the CLF-SSA algorithm, the model can dynamically lock onto the parameter combination that yields the optimal decomposition of the displacement sequence. This provides a robust foundation for the subsequent precise separation of step-like landslide displacement components.

2.3.3 Theoretical basis for physics-constrained evaluation

When processing step-like landslide displacements, minimizing mathematical sparsity metrics-such as the minimum envelope entropy (*Ep*)-does not inherently guarantee physical validity. Since landslide deformation is driven by hydrological triggers, the intrinsic physical logic mandates that the decomposed periodic modes maintain high statistical coherence with external driving forces, such as reservoir water levels or precipitation. This coherence can be quantitatively evaluated using the PCC:

$$\rho_{X,Y}=\frac{\mathrm{cov}(X,Y)}{\sigma_X\sigma_Y}=\frac{E[(X-\mu_X)(Y-\mu_Y)]}{\sigma_X\sigma_Y} \tag{6}$$

In this framework, covariance and standard deviation characterize the evolutionary consistency and normalization between displacement components and driving factors. This study asserts that the optimal solution must be synergistically constrained by both mathematical sparsity and physical coherence. Without robust physical constraints, optimization solely targeting entropy minimization is prone to over-decomposition. This can cause step-jump features—which share a unified physical mechanism—to be dispersed into unrelated modes, thereby stripping the results of their geomechanical interpretability.

2.4 Multi-dimensional IMF-like classification and reconstruction logic

Traditional displacement decomposition methodologies predominantly rely on simplistic frequency-based partitioning, which struggles to accurately identify the complex "reservoir-rainfall" nonlinear responses in step-like landslides (Jiang et al., 2024; Chen et al., 2025). Given the intense non-stationarity of step-like signals in the time-frequency domain, isolated metrics are insufficient to fully characterize the physical attributes of individual modes. Consequently, this study proposes a reconstruction framework driven by multi-dimensional features. By establishing a rigorous mapping between mathematical descriptors and physical evolutionary mechanisms, this approach aims to mitigate mode over-decomposition and resolve the ambiguity in physical interpretability.

- Identification of the Trend Component. Utilizing the low-pass filtering characteristics of VMD, components with near-zero central frequencies (ω_k), typically corresponding to multi-year evolutionary scales, are identified (Jiang et al., 2024). A modal component is classified as the trend displacement if it exhibits a monotonic increasing trajectory and maintains high correlation with the long-term geomorphological evolution of the slope.
- Identification of the Periodic Component. This involves aggregating modes that exhibit significant statistical coherence with hydrological triggers — such as reservoir level fluctuations and seasonal precipitation — or possess dominant

https://doi.org/10.5194/egusphere-2026-2913
Preprint. Discussion started: 6 August 2026

seasonal frequency signatures. These components reflect the step-like fluctuations induced by cyclical environmental perturbations.

- Identification of the Random Component. Based on information entropy theory, residual components characterized by high envelope entropy and high central frequencies are clustered as the random term. This component is validated through its association with high-frequency disturbances, such as extreme rainfall events, abrupt reservoir level shifts, and monitoring noise (Ren et al., 2025).

The aforementioned multi-dimensional identification and reconstruction mechanism facilitates a precise mapping from mathematical modes to physical components. This framework effectively deconstructs nonlinear and non-stationary landslide displacement signals into a trend component representing long-term evolution, a periodic component driven by environmental cycles, and a stochastic component reflecting instantaneous disturbances. By embedding geoscientific prior knowledge constraints into the parameter optimization phase and reinforcing physical interpretability during the reconstruction stage, this "quantification-driven" architecture not only enables the quantitative elucidation of the triggering mechanisms behind step-like landslides but also establishes a rigorous numerical foundation for developing robust landslide early-warning models.

3 Optimized VMD and IMF-like decomposition framework

To address the highly non-stationary and multi-scale coupling characteristics of step-like landslide displacement signals, this study develops an integrated adaptive VMD and physical reconstruction framework. Centered on Variational Mode Decomposition (VMD), the framework employs a Sparrow Search Algorithm enhanced by Chebyshev mapping and Lévy flight strategies (CLF-SSA) to automatically determine the optimal decomposition parameters—mode number k and penalty factor α. This approach effectively overcomes the subjectivity and mode-mixing issues inherent in traditional decomposition methods. Consequently, the raw cumulative displacement is decomposed into a series of IMF-like (Intrinsic Mode Function-like) components with distinct center frequencies.

3.1 Model architecture

This study develops a displacement decomposition framework utilizing a multi-stage cascading architecture—characterized by "data-driven optimization and physical-mechanism reconstruction" — to achieve the precise decoupling of step-like landslide displacements. As illustrated in Figure 1, the framework integrates three core functional modules: An adaptive parameter space search module based on the CLF-SSA algorithm, responsible for dynamically identifying the optimal decomposition parameters; a high-fidelity signal stripping module utilizing VMD to execute the variational decomposition of the raw sequence; and a multi-dimensional IMF-like classification and reconstruction module, which facilitates logical component aggregation via physical-mathematical feature mapping.

https://doi.org/10.5194/egusphere-2026-2913
Preprint. Discussion started: 6 August 2026

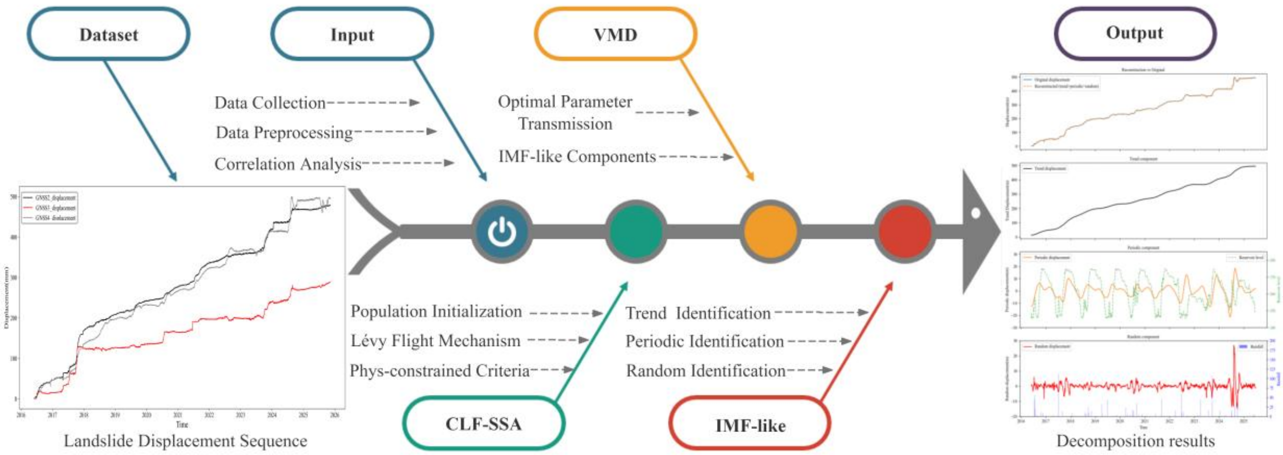

Figure 1: Figure 1. Architecture of the landslide displacement decomposition model based on CLF-SSA-VMD and IMF-like.

- Parameter Space Search Module (CLF-SSA). This module is responsible for exploring and identifying the optimal parameters ($k \in [3, 8]$, $\alpha \in [1000, 2500]$) within the predefined search space. To ensure the results align with geomechanical reality, a Joint Fitness Function is incorporated to embed physical constraints into the optimization process, as formulated in Eq. (7):

$$J(k, a) = \min\left(\mathrm{Mean}(EE) + \lambda \cdot \left(1 - \max(\rho_{resv})\right)\right) \tag{7}$$

In this formulation, $\mathrm{Mean}(EE)$ represents the average envelope entropy of all IMFs, utilized to suppress mode mixing and ensure the mathematical purity of signal decomposition. ρ_{resv} denotes the PCC between the IMF components and the reservoir water level sequence, while λ serves as the physical constraint weight factor.

By leveraging the Chebyshev mapping and Lévy flight mechanisms described in Section 2.3, the CLF-SSA algorithm achieves an optimal trade-off between mathematical sparsity (envelope entropy) and geological response coherence (PCC). Ultimately, it provides the VMD engine with the optimal parameter pair that yields the highest degree of geoscientific interpretability.

- Variational Signal Decomposition Module (VMD). As the core unit of signal decomposition, this module receives the optimal parameters transmitted from the preceding stage and performs a quasi-orthogonal decomposition of the raw cumulative displacement $X(t)$ within the spectral domain using the alternating direction method of multipliers (ADMM). The output consists of k^* independent IMF-like components, $\{u_1, u_2, \ldots, u_{k^*}\}$, which effectively capture and lock onto the deformation characteristics across diverse time scales.
- IMF-like Classification and Reconstruction Module. Guided by the IMF-like reconstruction logic detailed in Section 2.4, this module performs semantic identification and logical regrouping of the k raw modes by establishing "mathematical-physical" diagnostic criteria. Specifically, the trend component, reflecting long-term landslide creep, is

extracted based on frequency monotonicity and low-frequency evolutionary criteria; the periodic component, driven by
255 environmental forcing such as reservoir fluctuations and precipitation, is captured via a co-synergistic determination mechanism (Box et.al, 2015; Ren et.al, 2025); and the random component is formed by aggregating high-frequency residual sequences to characterize monitoring noise and impulsive environmental shocks. This reconstruction process facilitates a fundamental attribute transition from mathematical modes to geoscientific components, providing a rigorous basis for subsequent driving mechanism analysis.

260 **3.2 Operational workflow**

The specific execution procedure of the proposed model is outlined as follows (refer to Fig. 2 for the detailed flowchart).

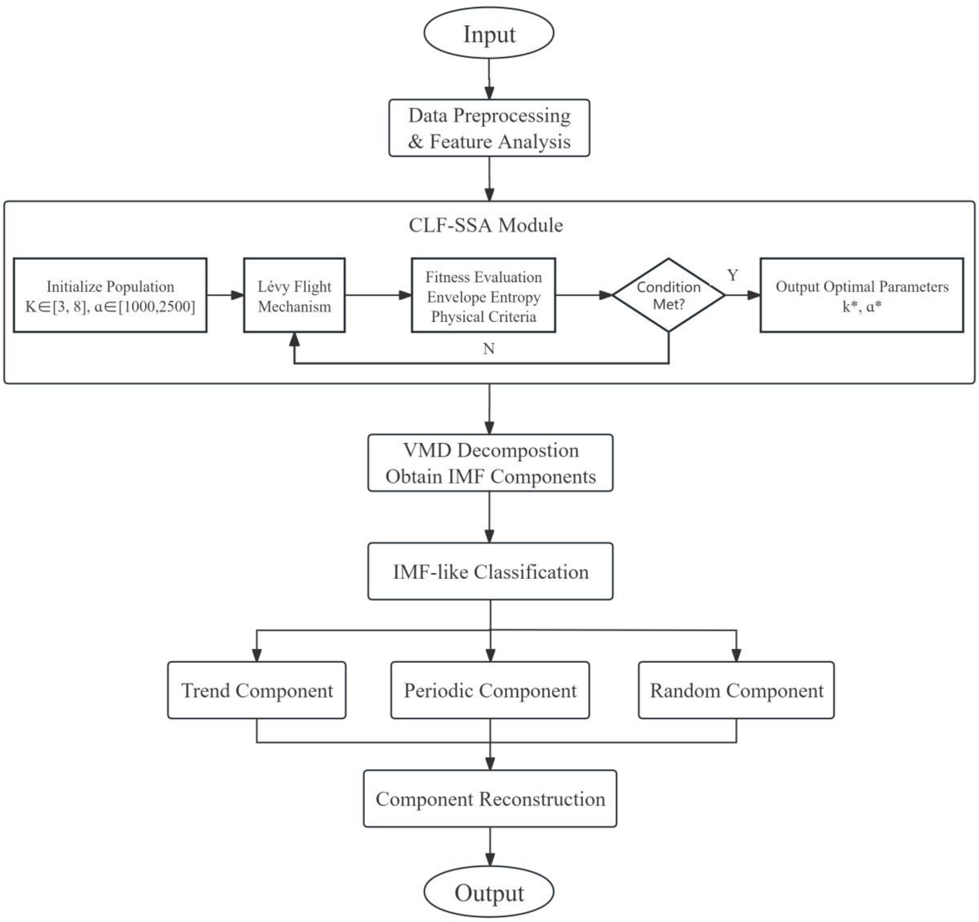

Figure 2: Operational flowchart of the CLF-SSA-VMD model integrated with the IMF-like reconstruction framework.

https://doi.org/10.5194/egusphere-2026-2913
Preprint. Discussion started: 6 August 2026

- Step 1: Data initialization and pre-processing. The landslide monitoring dataset, comprising cumulative displacement, reservoir levels, and precipitation, is imported. Data normalization is performed according to the criteria in Section 2.4, and the initial time-series mapping between environmental drivers and total displacement is established.
- Step 2: Adaptive parameter searching (CLF-SSA Module). The enhanced Sparrow Search Algorithm is initiated to iterate within the parameter space. The fitness of each generation is evaluated by the physics-constrained criteria (Eq. 6). The Chebyshev map ensures the ergodicity of the initial search, while the Lévy flight mechanism forces the algorithm to escape local extrema traps, ultimately locking onto the global optimal parameter pair $\left(k^*, a^*\right)$.
- Step 3: Variational decomposition (VMD Module). The optimal parameters are fed into the VMD engine to execute narrow-band decomposition. This stage outputs k^* independent IMF-like modes, facilitating the smooth transfer of energy from the raw signal to diverse frequency components while effectively suppressing edge effects caused by parameter mismatch.
- Step 4: Multi-dimensional identification and reconstruction. Multi-dimensional diagnostic criteria-including frequency monotonicity, hydrological response coherence, and seasonal energy ratios-are applied for the automated semantic classification of the k^* modes. These modes are then aggregated into the trend, periodic, and stochastic components.
- Step 5: Model output and validation. The three displacement components with distinct physical meanings are generated. The reconstruction residuals are validated to ensure they meet precision requirements, providing a high-quality, feature-rich input set for subsequent landslide prediction modeling.

4 Field investigation and data preparation

The Yutang landslide, situated on the right bank of the Yangtze River in Yunyang County, Chongqing of China, is a representative consequent soil-like reservoir landslide within the TGR area . The landslide exhibits pronounced step-like deformation characteristics, with its evolutionary process synergistically controlled by both reservoir water level fluctuations and seasonal precipitation. Its complex nonlinear response mechanism makes it an ideal case study for validating the optimized VMD decomposition model proposed in this research.

4.1 Study area overview

The toe of the Yutang landslide extends directly into the main channel of the Yangtze River. The site is characterized by typical denudation-hills geomorphology, with a topographic gradient sloping from south to north at inclinations ranging from 16° to 25°. Due to long-term fluvial erosion by the Yangtze River, prominent erosional scarps and floodplains have developed at the landslide's front edge, while the rear boundary is defined by bedrock cliffs 8 – 15 m in height. The micro-topography exhibits distinct features, including a free face at the front, a broad platform in the central section, and gentle terrain at the rear.

https://doi.org/10.5194/egusphere-2026-2913
Preprint. Discussion started: 6 August 2026

Geologically, the landslide is a representative consequent soil-like slope. As illustrated in Fig. 3, the landslide exhibits a tongue-shaped planar morphology with a primary sliding direction of 341°. It has a longitudinal length of approximately 700 m and a transverse width varying between 150 and 400 m. With an average sliding mass thickness of 20 m and a total volume of approximately 3.20×10^6 m³, it is classified as a large-scale consequent soil-like reservoir landslide. The landslide boundaries are well-defined: laterally incised by gullies, rear-bounded by steep bedrock walls, and front-extended below the perennial reservoir water level. This unique consequent structure, coupled with the hydro-fluctuation environment, renders its displacement evolution highly sensitive to reservoir level fluctuations and precipitation forcing.

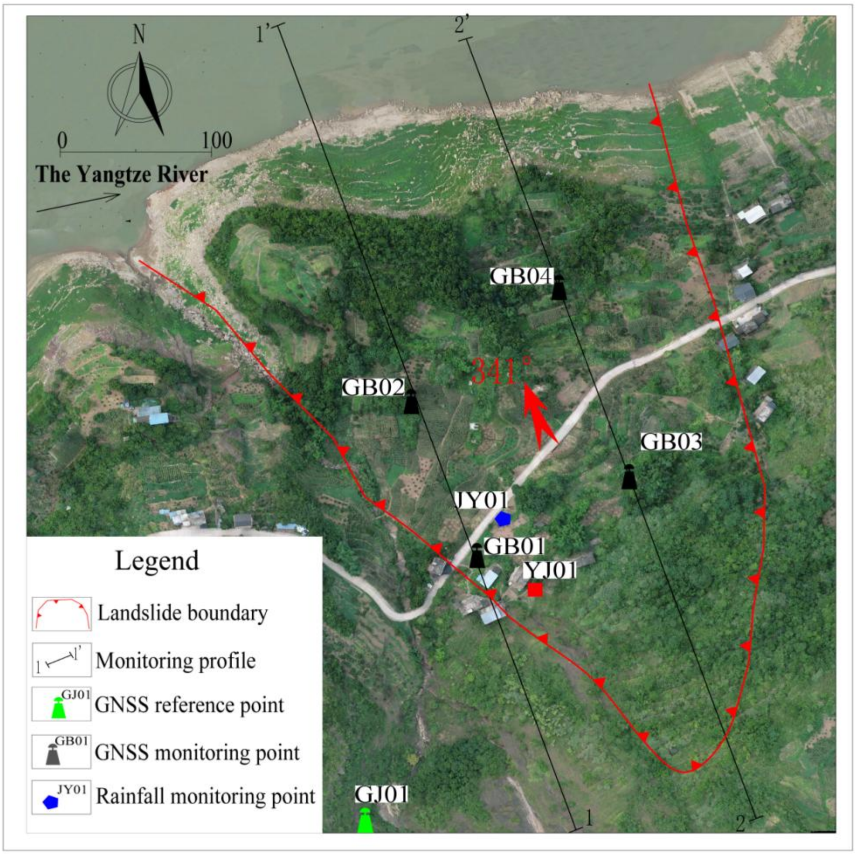

Figure 3: Orthophoto map and distribution of monitoring stations for the Yutang landslide.

4.2 Data collection and visualization

Based on the fundamental geomorphological features and deformation characteristics of the Yutang landslide, a comprehensive multi-parameter monitoring system was implemented. The core of this system focuses on landslide surface displacement monitoring, integrated with the synchronized tracking of reservoir water level fluctuations and seasonal precipitation. The detailed specifications of the monitoring program are summarized in Tab. 2. This configuration is

https://doi.org/10.5194/egusphere-2026-2913
Preprint. Discussion started: 6 August 2026

designed to provide high-dimensional time-series data, enabling the refined characterization of the landslide's dynamic response processes.

Table 2 Table of the landslide monitoring contents

No.	Monitoring content	Function
1	Landslide surface displacement	Obtain the three-dimensional displacement changes by GNSS
2	Rainfall	Obtain daily cumulative rainfall within the landslide area
3	Reservoir water level	Obtain changes in reservoir water at the landslide front.

This paper collects landslide monitoring data for 10 years (June 2016 to November 2025), and the monitoring curves are shown in Fig. 4.

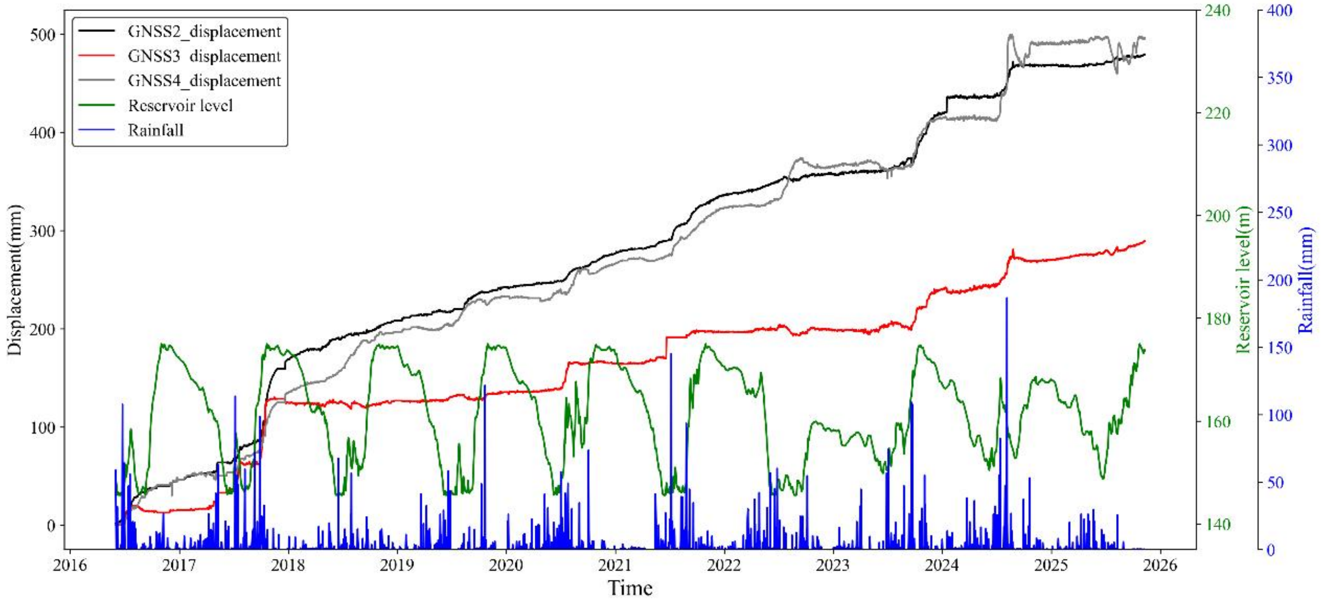

Figure 4: **Display of horizontal displacement monitoring data of the GNSS points**

As illustrated in Fig. 4, the cumulative displacement of the landslide exhibits pronounced non-stationary and multi-scale step-like characteristics.

- Seasonal surges. From May to September annually, synchronized with rapid reservoir drawdown and frequent heavy rainfall, the displacement curves exhibit significant "step-jump" accelerations. During the summers of 2021 and 2023, the instantaneous displacement rates at GNSS3 showed particularly dramatic increments.
- Evolutionary staging. During periods of high-level reservoir operation, the displacement enters a relatively stable "stagnation plateau," characterized by extremely low-frequency long-term creep trends.

https://doi.org/10.5194/egusphere-2026-2913
Preprint. Discussion started: 6 August 2026

- Multi-field coupling and lag effects. The displacement jump points exhibit strong statistical coherence with the rate of reservoir drawdown and precipitation peaks in the time series; however, this correlation is governed by complex nonlinear lag effects.

The structural complexity of monitoring signals—marked by multi-scale non-stationarity and inherent spectral overlap—renders conventional linear analysis insufficient for achieving rigorous causal decoupling. To overcome this limitation, the implementation of a physics-constrained Optimized VMD framework is imperative, as it enables the precise extraction of periodic responses and ensures the orthogonal isolation of driving mechanisms from coupled displacement sequences.

5 Experimental results

To validate the effectiveness of the proposed Optimized VMD and IMF-like framework in decomposing step-like landslide displacements, this chapter provides an empirical analysis using the Yutang landslide as a representative case.

5.1 Results of Adaptive Parameter Optimization

Prior to signal decomposition, the enhanced CLF-SSA algorithm was employed to perform an adaptive search for the optimal parameter pairs across the displacement sequences of three representative monitoring stations (GNSS2, GNSS3, and GNSS4). Table 3 summarizes the optimization results, where k^* denotes the optimal number of Intrinsic Mode Functions (IMFs) derived from the VMD process, and a^* represents the quadratic penalty factor governing the bandwidth of the decomposed components.

Table 3. Table of VMD Decomposition Parameters $\left(k^*, a^*\right)$

Monitoring Point	k^*	a^*
GNSS2	4	979.66
GNSS3	6	1273.78
GNSS4	6	1405.60

The results in Tab. 3 demonstrate that the proposed algorithm can dynamically identify the most suitable parameter combinations based on the unique signal characteristics of each station, thereby establishing a rigorous mathematical foundation for subsequent physical component extraction.

A comparative analysis reveals significant discrepancies in the optimal parameter combinations $\left(k^*, a^*\right)$ across different monitoring stations, uncovering the spatiotemporal heterogeneity of deformation dynamics during landslide evolution.

- Disparity in deformation mechanism complexity: Both GNSS2 and GNSS4 are located within the primary sliding zone exhibiting intense deformation, with cumulative displacements significantly exceeding other stations. However, the K value for GNSS4 (k^*) is higher than that of GNSS2 (k^*), suggesting a more intricate composition in the GNSS4

https://doi.org/10.5194/egusphere-2026-2913
Preprint. Discussion started: 6 August 2026

signal. This indicates that beyond long-term creep and hydrological responses, GNSS4 incorporates richer subtle step-jumps or stochastic fluctuations, whereas GNSS2 exhibits more concentrated energy distribution and a purer deformation mechanism.

- Necessity of Higher Modal Order: The optimal k^* value for both GNSS3 and GNSS4 is identified as 6. A higher modal order ensures that during complex "step-jump" transition periods, high-frequency rainfall pulse responses remain effectively decoupled from mid-frequency reservoir level responses without mode mixing, thereby providing high-purity characteristic modes for subsequent physical component extraction.
- Rationality and Physical Significance of the Penalty Factor: The optimized a^* values range between 980 and 1406, an interval that demonstrates high rationality in both mathematical resolution and physical mechanisms (Dragomiretskiy and Zosso, 2013). This range effectively suppresses mode mixing while preserving the sharp "step-like" transient features of the displacement curves. Furthermore, it ensures significant statistical coherence between the decomposed modes and reservoir water level fluctuations. These results, driven dually by mathematical sparsity and physical correlation, confirm that the model has successfully converged into the global optimal solution space.

5.2 Analysis of displacement decomposition results

Based on the aforementioned optimal parameter combinations (k^*, a^*), the VMD algorithm was executed to perform high-fidelity narrow-band decomposition of the cumulative displacement sequences for each monitoring station. The resulting decomposed IMF components and their correspondence with the raw signals for stations GNSS2, GNSS3, and GNSS4 are illustrated in Fig. 5, Fig. 6, and Fig. 7, respectively.

https://doi.org/10.5194/egusphere-2026-2913
Preprint. Discussion started: 6 August 2026

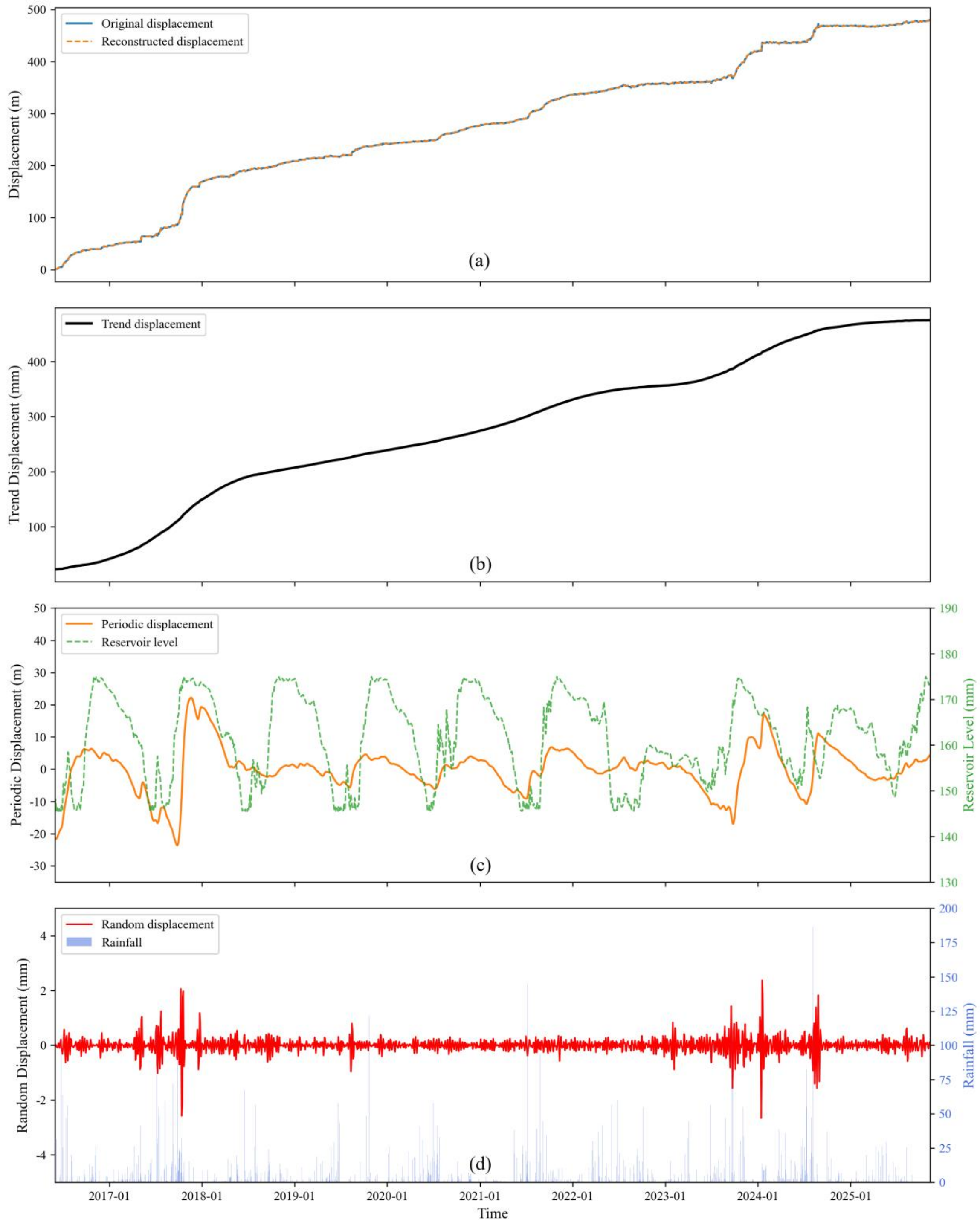

Figure 5: Multi-component decomposition results of the cumulative displacement of GNSS2.

370

https://doi.org/10.5194/egusphere-2026-2913
Preprint. Discussion started: 6 August 2026

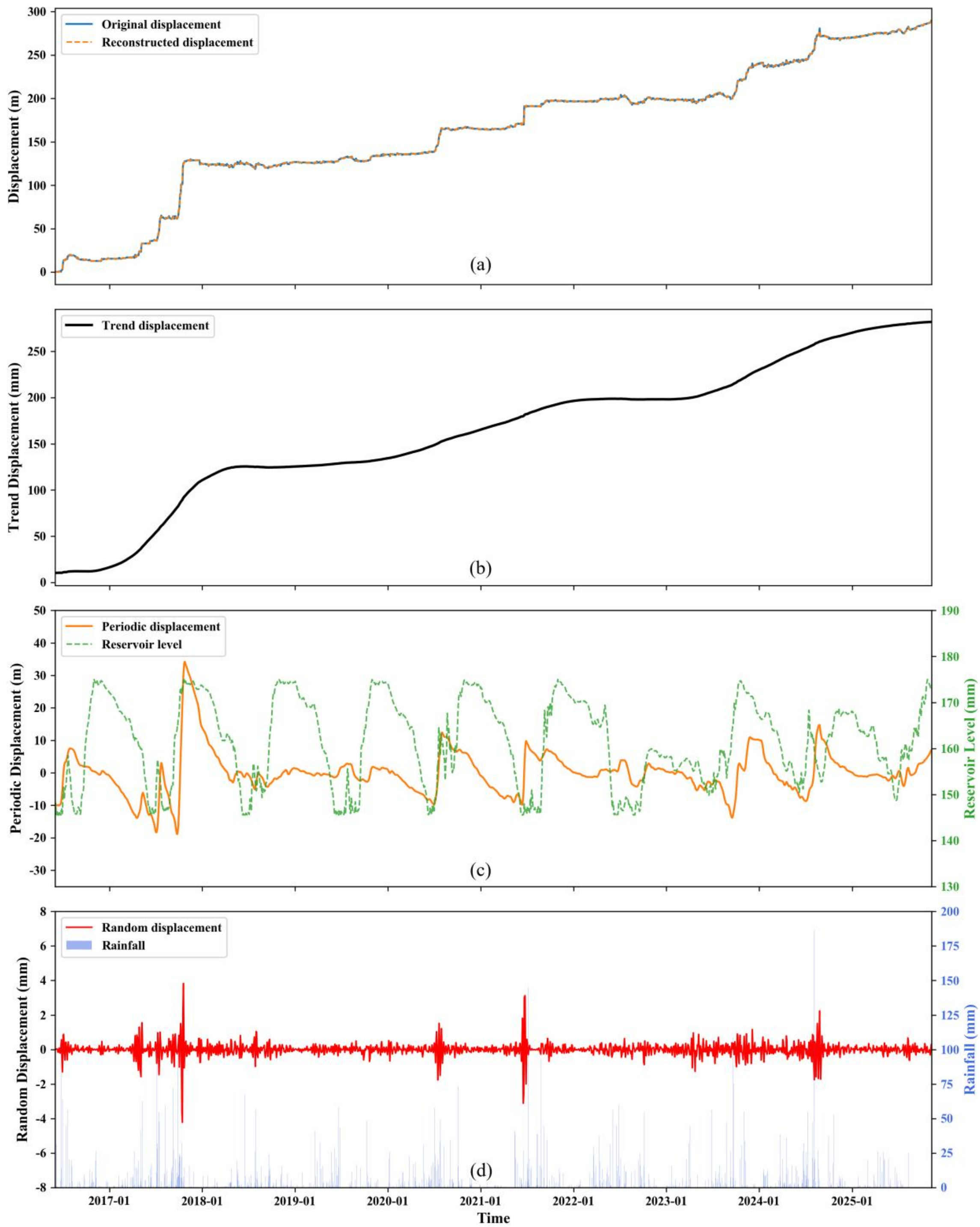

Figure 6: Multi-component decomposition results of the cumulative displacement of GNSS3.

https://doi.org/10.5194/egusphere-2026-2913
Preprint. Discussion started: 6 August 2026

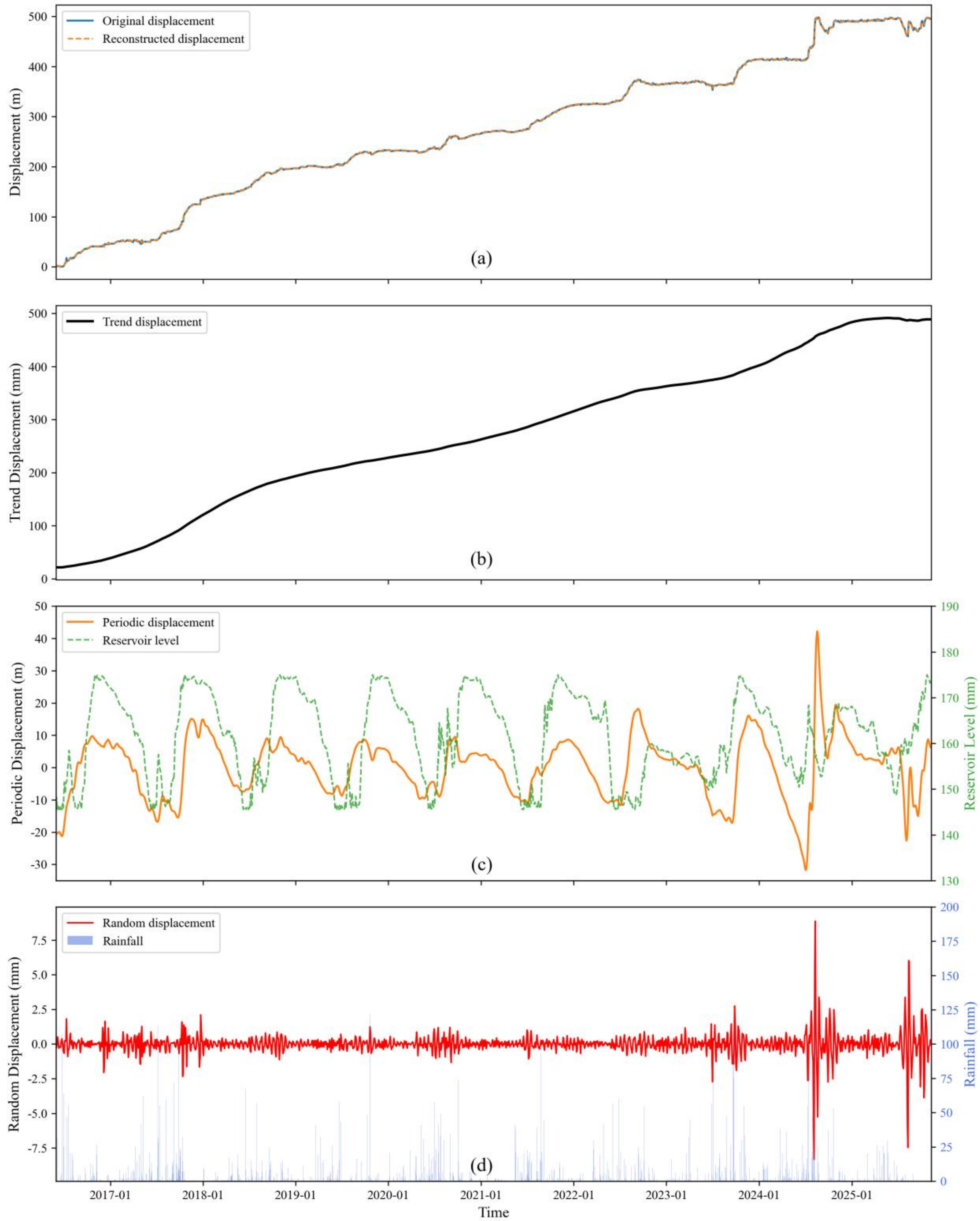

Figure 7: Multi-component decomposition results of the cumulative displacement of GNSS4.

https://doi.org/10.5194/egusphere-2026-2913
Preprint. Discussion started: 6 August 2026

The decomposition results in Figure 5-7 explain:

- Reconstruction fidelity and adaptivity. Experimental results confirm the superior reconstruction accuracy of the proposed framework. As shown in Figs. 3(a) – 5(a), the reconstructed curves—synthesized from the trend, periodic, and stochastic components—exhibit high statistical coherence with the raw trajectories. This demonstrates that the CLF-SSA-driven VMD accurately identifies center frequencies, minimizing energy dissipation and preserving the quintessential non-stationary "step-like" features at the numerical level.
- Trend component and evolutionary essence. The trend components (Figs. 3(b) – 5(b)) quantitatively characterize the long-term evolution governed by intrinsic geological conditions. Represented as a monotonically increasing nonlinear creep, the trend successfully identifies acceleration inflections driven by internal dynamics. By optimizing the penalty factor α, the framework effectively filters high-frequency noise while maintaining curvature smoothness and evolutionary continuity, accurately reflecting the baseline deformation under gravitational accumulation.
- Periodic component and hydrological response. The periodic components (Figs. 3(c) – 5(c)) reveal the sensitivity of displacement to hydrological triggers. The observed seasonal oscillations are highly synchronized with reservoir water level (RWL) cycles. Specifically, the alignment of periodic peaks with reservoir drawdown phases confirms that seepage force increments are the primary drivers of seasonal accelerations. This further validates the "physical correlation + seasonal energy ratio" criteria for isolating subtle response modes amidst complex background noise.
- Stochastic component and instantaneous perturbations. The stochastic components (Figs. 3(d) – 5(d)) precisely map the instantaneous impacts of extreme meteorological events. During heavy rainfall windows, this component manifests as distinct short-term pulses, with amplitudes correlating positively with rainfall intensity. The successful decoupling of these aperiodic disturbances underscores the robustness of the proposed architecture in handling coupled multi-source signals.

5.3 Quantitative verification of component decoupling

To quantitatively evaluate the reliability of the Optimized VMD-IMF-like framework in isolating physical components, PCC were employed to verify the consistency between reconstructed components and core triggering factors. Table 4 summarizes the verification results for the three representative monitoring stations.

Table 4. Quantitative verification of decomposed components and environmental triggers.

Monitoring Point	Original Pearson	Decomposed Pearson	Improvement	Trend Monotonicity	RMSE (mm)
GNSS2	0.0155	0.4849	+3024.28%	0.9883	0.4353
GNSS3	0.0321	0.3140	+876.97%	0.9730	0.4486
GNSS4	0.0103	0.4496	+4283.60%	0.9938	0.5667

https://doi.org/10.5194/egusphere-2026-2913
Preprint. Discussion started: 6 August 2026

5.3.1 Correlation enhancement with hydrological drivers

The most significant breakthrough in the decomposition results is the magnitude-order enhancement in the correlation between reconstructed periodic displacement and the reservoir water level. As indicated in Tab. 4, the original cumulative displacement exhibits extremely low PCC values with RWL (ranging from 0.0103 to 0.0321) due to the overwhelming dominance of the long-term trend component.

Following the implementation of the proposed model, the correlation for the periodic components exhibits an "explosive" growth, with GNSS4 achieving an improvement of 4283.60%. This demonstrates that the physics-constrained criteria, by dually constraining mathematical sparsity and physical coherence, successfully decouples the periodic physical response triggered by reservoir operations from complex non-stationary signals.

5.3.2 Monotonicity and numerical fidelity analysis

The analysis further shows that the linear correlation between the trend components and the time series ranges from 0.9730 to 0.9938. This high degree of linearity quantitatively proves that the trend components effectively strip away seasonal fluctuations and stochastic pulses, accurately delineating the monotonic evolutionary trajectory driven by intrinsic geological factors.

Furthermore, the model demonstrates superior numerical precision: the correlation between the reconstructed and original sequences remains above 0.9999, with the RMSE strictly controlled between 0.435 and 0.567 mm. Given the cumulative displacement magnitude (~500 mm), this error ratio is negligible, validating that the physics-guided reconstruction logic maintains high numerical fidelity while capturing the essential geomechanical characteristics.

6 Discussion

The decomposition framework developed in this study not only achieves superior numerical precision but also elucidates the intrinsic decoupling potential of the evolutionary patterns in step-like landslides from a mechanistic perspective. To further validate the physical rationality and engineering applicability of the proposed model, the discussion provides an in-depth discussion focusing on the following dimensions: First, an objective evaluation of the adaptive boundaries and uncertainties of the model under fluctuating environments is conducted to quantify its robustness amidst dynamic and complex geological conditions. Subsequently, a continuous-slip numerical model is constructed to facilitate a comparative analysis between the simulation results-governed by quasi-physical constitutive laws-and the decomposed components. This approach establishes a closed-loop analytical transition from observational data to numerical simulation, effectively advancing the research from statistical feature identification to a rigorous interpretation of physical mechanisms.

https://doi.org/10.5194/egusphere-2026-2913
Preprint. Discussion started: 6 August 2026

6.1 Model robustness and uncertainty assessment

Within complex natural geological environments, the identification, monitoring, and early warning of landslides are inevitably confronted by challenges arising from multifaceted uncertainties (Casagli et al., 2023). Traditional paradigms for analyzing step-like landslides predominantly rely on threshold criteria of cumulative displacement or its derivative indices, such as displacement velocity and tangent angles (Intrieri et al., 2012; Segoni et al., 2018; Wu et al., 2025). However, these methods often struggle with the dual dilemma of signal interference and physical decoupling when processing highly non-stationary sequences. Although the displacement decomposition framework proposed in this study exhibited superior performance in the empirical analysis of the Yutang landslide (in Chapter 5), a profound investigation into its robustness boundaries under dynamic environments remains essential.

6.1.1 Statistical significance and correlation with environmental triggers

Model uncertainty primarily stems from the complex nonlinear mapping between external triggers and slope response. Existing studies suggest that geohazard models often exhibit predictive biases due to incomplete forcing data or insufficient representation of internal variability (Pecoraro et al., 2019; Bjordal et al., 2026). Although this study, within a physics-informed paradigm, establishes strong correlations between displacement components and core triggers (reservoir levels and precipitation) via physics-constrained criteria, landslide evolution remains an inherently multi-field coupled process (Bradley et al., 2019). Beyond hydrodynamic drivers, the inadequate representation of factors such as geostructural evolution, seismic loading, and deep groundwater dynamics may still pose risks of incomplete mechanistic coverage under extreme operating conditions.

Drawing upon the decomposition results of the Yutang landslide, this section analyzes the \$p\$-values representing the statistical significance of the periodic component relative to reservoir levels and the stochastic component relative to precipitation. This analysis aims to comprehensively elucidate the discrepancies in the model's identification capacity and robustness across heterogeneous physical triggers. The statistical verification results for the three monitoring stations are summarized in Tab. 5.

Table 5. statistical significance of decomposed components and their environmental triggers

Monitoring point	Index	Periodic vs. RWL	Random vs. Rainfall
GNSS2	*p*-value	5.11×10^{-203}	5.45×10^{-3}
GNSS3	*p*-value	8.09×10^{-80}	2.38×10^{-13}
GNSS4	*p*-value	2.41×10^{-171}	2.07×10^{-9}

Integrated discussion:

- Significance validation of dual triggers. As indicated in Tab. 5, both periodic and stochastic components exhibit highly significant statistical correlations ($p<0.001$) across all stations. This not only confirms reservoir levels and rainfall as

https://doi.org/10.5194/egusphere-2026-2913
Preprint. Discussion started: 6 August 2026

the primary drivers of periodic steps and random perturbations, respectively, but also statistically eliminates the possibility of "mathematical fitting artifacts," thereby reinforcing the robustness of the proposed framework.

- Magnitude disparity between deterministic and stochastic responses. The *p*-values for periodic components are orders of magnitude smaller than those for stochastic ones, reflecting a fundamental distinction: reservoir-induced deformation is characterized by high determinism and synchronicity, whereas rainfall-triggered responses involve greater uncertainty due to nonlinear processes such as seepage lag and saturation thresholds.
- Statistical robustness against environmental noise. The exceptional statistical significance suggests that the core physical laws captured by the model remain dominant. Even with incomplete forcing data, the framework effectively mitigates identification uncertainties arising from unmeasured factors (e.g., deep pore-water pressure) by prioritizing strongly correlated feature extraction.

6.1.2 Model fidelity and structural robustness

Numerical reconstruction fidelity serves as a critical dimension for evaluating model robustness. Following the assessment paradigms of Earth system modeling (e.g., NorESM2-DIAM (Bjordal et al., 2026)), the ability to capture observational extrema and abrupt transitions directly dictates predictive credibility. In this framework, the overall reconstruction correlation consistently exceeds 0.9999, with the RMSE strictly confined between 0.435 and 0.567 mm. Such negligible errors—at the scale of one-thousandth of the total displacement—demonstrate superior structural stability in processing non-stationary "step-like" features. While the stochastic component's correlation remains relatively lower due to landslide response lag, the exceptional fidelity ensures that anomalous surges are accurately preserved even under extreme rainfall, thereby mitigating the risk of false alarms (in Tab. 6).

Table 6. Evaluation of numerical fidelity for the reconstructed displacement sequences.

Monitoring point	RMSE (mm)	Correlation coefficient	Error percentage
GNSS2	0.4353	0.999995	0.087%
GNSS3	0.5674	0.999982	0.113%
GNSS4	0.4938	0.999992	0.098%

Integrated discussion:

- Precision control of reconstruction errors. As shown in Tab. 6, the RMSE for displacement reconstruction is strictly maintained within the sub-millimeter range (0.435–0.567 mm). Against a total cumulative displacement exceeding 500 mm, the relative error is approximately 0.1%. This high fidelity ensures that local abrupt transitions with early-warning value are not misidentified as noise during the extraction of low-frequency components, providing quantitative evidence for model robustness.

https://doi.org/10.5194/egusphere-2026-2913
Preprint. Discussion started: 6 August 2026

- Fidelity of non-stationary "Step-like" features. Step-like landslides exhibit intense non-stationarity. Traditional smoothing or decomposition algorithms often suffer from spurious oscillations or over-smoothing at inflection points, leading to the loss of critical dynamic features. The near-unity correlation between the reconstructed and original sequences demonstrates that the CLF-SSA-optimized VMD framework accurately preserves step-jump characteristics, effectively preventing the loss of warning information due to structural deficiencies.
- Mitigation of parameter sensitivity uncertainties. In conventional decomposition methods, minor variations in k and α often cause drastic fluctuations in output. By employing the physics-constrained evaluation mechanism for parameter optimization, the proposed model maintains stable and minimal reconstruction errors across diverse monitoring stations and local geological settings. This consistent performance across spatial locations eliminates the risk of overfitting to specific datasets, reflecting superior structural stability and generalizability.

6.2 Physical mechanism validation

This section implements a PyLith-based continuous-slip numerical model (Aagaard et al., 2017) to establish a closed-loop analytical framework that bridges "observational data-driven decomposition" and "numerical constitutive simulation." By comparing the periodic components isolated by the proposed model with the slope responses simulated via porous media seepage theory, the dynamic contribution rates of reservoir drawdown and heavy rainfall pulses across different evolutionary stages are quantitatively elucidated.

6.2.1 Model setup based on continuous slip representation

In the numerical modeling, the Yutang landslide is conceptualized as a block system undergoing shear movement along the sliding surface, with its deformation driven by prescribed piecewise constant slip rates. Deviating from traditional instantaneous slip assumptions, this study employs a continuous slip representation to characterize the landslide evolution. The primary sliding surface is partitioned into five sub-zones along the main sliding direction, each assigned distinct slip rates to reflect spatial heterogeneity in deformation. Temporally, all segments initiate simultaneously and evolve throughout the simulation period, forming a continuous cumulative displacement process. This setup effectively maps the trend components derived from time-series decomposition onto the slip-rate distribution, facilitating the transition from a data-driven model to a physical process model.

https://doi.org/10.5194/egusphere-2026-2913
Preprint. Discussion started: 6 August 2026

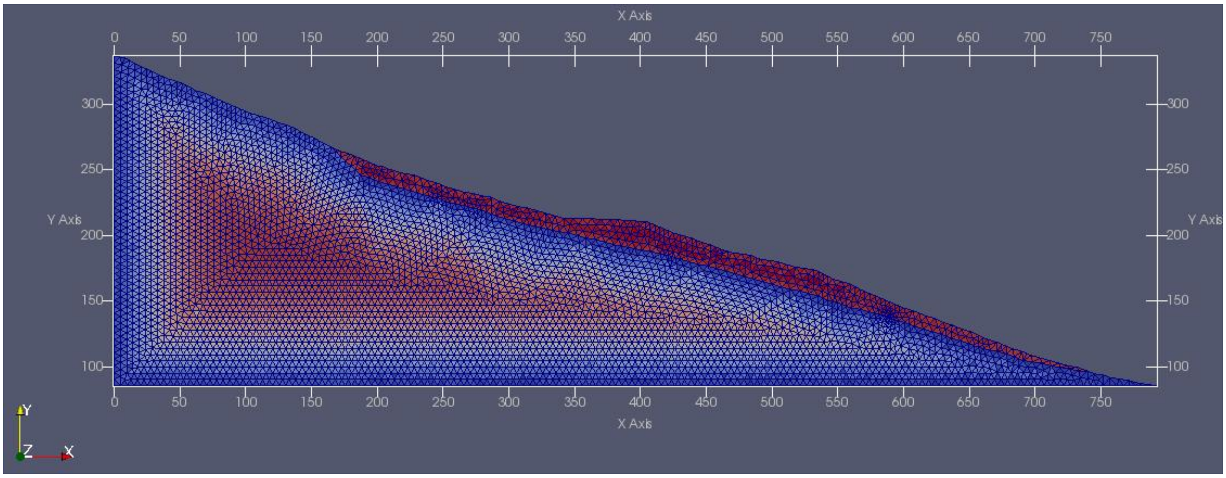

Figure 8: Model of the Yutang landslide setup.

As illustrated in Fig. 8, the numerical mesh comprises 4,077 nodes and 7,784 triangular elements, covering a horizontal extent of 0–792 m and an elevation range of 86–336 m. Guided by borehole data, the sliding surface (fault) is embedded with a 19° dip (340°∠19°) and discretized into 115 nodes. Constraints are applied to the slope surface, bottom, and left boundaries. To implement a data-driven approach, cumulative horizontal displacements from stations GB03 and GB04 in Fig. 3 are interpolated via a distance-weighted Green's function kernel to prescribe Dirichlet displacement boundary conditions for each node along the fault (Fig. 9(a)). This method transforms discrete observations into a continuous, spatially varying slip field, effectively mitigating the biases inherent in uniform slip-rate assumptions.

6.2.2 Model setup based on continuous slip representation

Fig. 9(a) displays the cumulative displacement field derived from the PyLith model at the end of the monitoring period (June 2025). The high-displacement zone (>490 mm) is concentrated in the mid-to-lower section of the landslide (elevation 140–210 m), aligning closely with the observed value at GB04 (496.0 mm). The simulated ratio of downslope to upslope displacement (≈1.79) matches the measured ratio, accurately reproducing the spatial heterogeneity of the deformation. Displacement vectors exhibit a deflection along a 19° dip, characterized by dominant horizontal movement and downward vertical components, consistent with typical bedding-controlled sliding kinematics. Notably, the displacement field attenuates significantly at the landslide toe (below 600 m) due to the lateral confining pressure from the TGR area , reflecting a local stabilization effect. Figs. 7(b) and 7(c) further illustrate the high temporal consistency between the observed and simulated displacement sequences for stations GB03 and GB04.

https://doi.org/10.5194/egusphere-2026-2913
Preprint. Discussion started: 6 August 2026

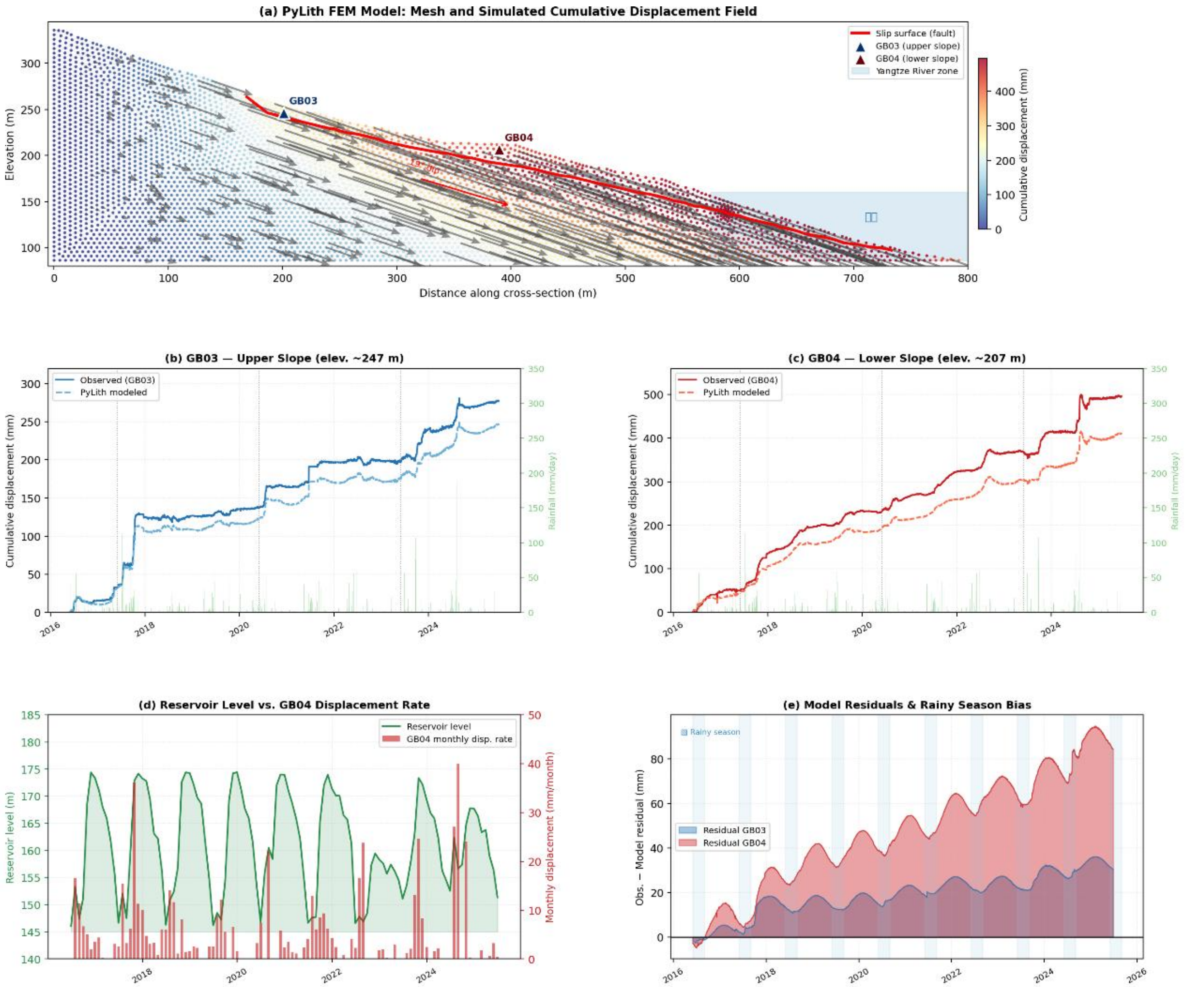

Figure 9: The Yutang landslide (Yunyang County, Three Gorges) simulation and GNSS observations.

Fig. 9 elucidates the high degree of spatiotemporal consistency between the numerical simulation and GNSS observations, thereby validating the mechanical interpretability of the proposed decomposition framework.

- Spatial distribution characteristics of the displacement field. Fig. 9(a) illustrates the cumulative displacement field of the landslide at the end of the monitoring period (June 2025). The high-displacement zone (>490 mm) is concentrated in the mid-to-lower section of the landslide body (stations 390 – 600 m, elevation 140 – 210 m), aligning closely with the observed value at GB04 (496.0 mm). The simulated ratio of downslope to upslope displacement (≈1.79) accurately reproduces the spatial heterogeneity of the deformation. Displacement vectors predominantly deflect along a 19° dip, exhibiting typical bedding-controlled sliding kinematics dominated by horizontal movement with downward vertical

https://doi.org/10.5194/egusphere-2026-2913
Preprint. Discussion started: 6 August 2026

components. Notably, the displacement field at the landslide toe attenuates significantly due to the lateral confining pressure from the TGR area , reflecting the localized stabilization effect of the reservoir water on the slope foot.

- Temporal Evolution and Reproduction of "Step-like" Features. Figs. 9(b) – 9(e) present the evolutionary patterns of displacement over the ten-year monitoring period. The model clearly delineates the "step-jump" accelerations: a period of gradual growth prior to 2018, a primary acceleration phase during 2020 – 2022 triggered by consecutive heavy rainfall years (e.g., the historic 2020 flood peak), and a secondary acceleration phase during 2023 – 2024, with the peak rate occurring in August 2024 (GB04 incrementing by ~45 mm/month). Quantitative verification metrics (Figs. 3a, 3b) show that the R^2 for stations GB03 and GB04 reach 0.998 and 0.999, respectively, with NRMSE values consistently below 12%. These indices demonstrate that the fault-slip boundary conditions extrapolated from dual-station GNSS data are highly representative, and the PyLith model effectively captures the long-term evolutionary trajectory of the landslide.
- Residual characteristics and limitations of the physical mechanism. Residual analysis (Fig. 3(e)) reveals a significant systematic positive bias during the annual rainy season (June – September), suggesting that the observed peak accelerations transcend the limits of linear elastic response. This discrepancy is primarily attributable to complex nonlinear mechanisms triggered by rainfall infiltration: firstly, the transient elevation of pore-water pressure induces "strength softening" along the sliding surface, a nonlinear strength evolution not incorporated in the current elastic framework; secondly, precipitation activates viscoelastic rheological behavior within the loose accumulation layers, exceeding the representative capacity of an elastic constitutive model. Notably, the residual amplitude at GB04 is approximately 2.4 times that of GB03, which is highly consistent with its lower elevation, closer proximity to the reservoir's hydrodynamic fluctuation zone, and more intense pore-pressure response, further confirming that hydrologically-driven nonlinear deformation is the primary source of model deviation.
- Dynamic response to reservoir hydrodynamic coupling. Fig. 9(d) elucidates the dynamic coupling between displacement rates and reservoir water levels. The rapid drawdown periods (April – June, 175 m to 145 m) correspond to phased accelerations in displacement, which is consistent with the mechanical mechanism where seepage forces act outward during reservoir drainage. Conversely, the high-level operation periods (September – November) exhibit a deceleration in displacement, reflecting the supporting effect of the reservoir's lateral pressure. While the model qualitatively reproduces this "drawdown-acceleration and impoundment-deceleration" effect through time-varying pressure boundaries, the quantitative magnitude remains approximately 18% lower than observed values. This discrepancy suggests that future work should incorporate more sophisticated saturated-unsaturated seepage coupling mechanisms.

https://doi.org/10.5194/egusphere-2026-2913
Preprint. Discussion started: 6 August 2026

6.2.3 Temporal evolution and phased characteristics of slope deformation

Figure 10 illustrates the evolution of the displacement field across four key temporal nodes (2018, 2020, 2022, and 2024), clearly elucidating the characteristic "step-like" acceleration of the landslide.

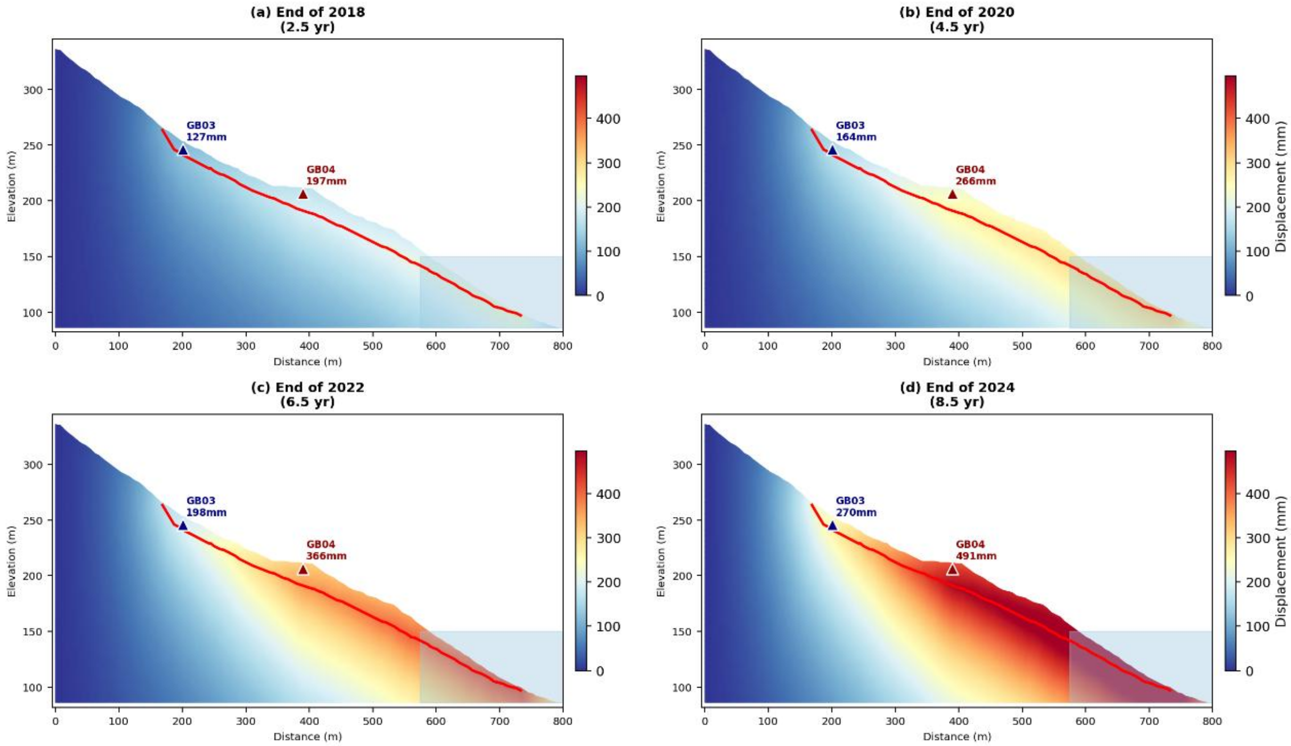

Figure 10: Temporal evolution of simulated displacement field.

The evolutionary process can be categorized into three distinct phases:

- Prior to late 2018, the displacement remained minimal with a gentle growth rate, representing a relatively stable creep phase.
- The first significant acceleration occurred during 2020 – 2022, which closely correlates with consecutive heavy rainfall events, such as the historic 2020 flood peak in the Three Gorges area.
- A second intense acceleration phase emerged during 2023 – 2024, with the velocity peaking in August 2024 (GB04 recorded a monthly increment of ~45 mm).

This step-wise pattern is accurately reproduced in the simulated displacement field, substantiating that the transient elevation of pore-water pressure triggered by intense rainfall is the direct driver of displacement surges, while periodic reservoir water level fluctuations further modulate the long-term stress state of the slope.

Figure 11 illustrates the evolution of the displacement profile along the slope surface. The profiles across all periods exhibit peak values between chainage 350 – 500 m, corresponding to the "bulging zone" in the middle of the landslide, which aligns

https://doi.org/10.5194/egusphere-2026-2913
Preprint. Discussion started: 6 August 2026

closely with the slip vectors in the numerical model. The gradual downslope migration of the peak displacement zone suggests a progressive advancement of the landslide front toward the toe; notably, the loss of reservoir water support at the toe could trigger further acceleration risks. These characteristics exhibit high consistency with the trend components derived from the displacement decomposition. While the trend represents the long-term evolutionary behavior, the prescribed continuous slip rate in the numerical model serves as its physical manifestation. Although minor discrepancies exist due to the simplified constant-rate assumption, the model's ability to reproduce the overall deformation magnitude over long-term scales validates the reliability of the "data-driven decomposition to physical-constitutive verification" framework.

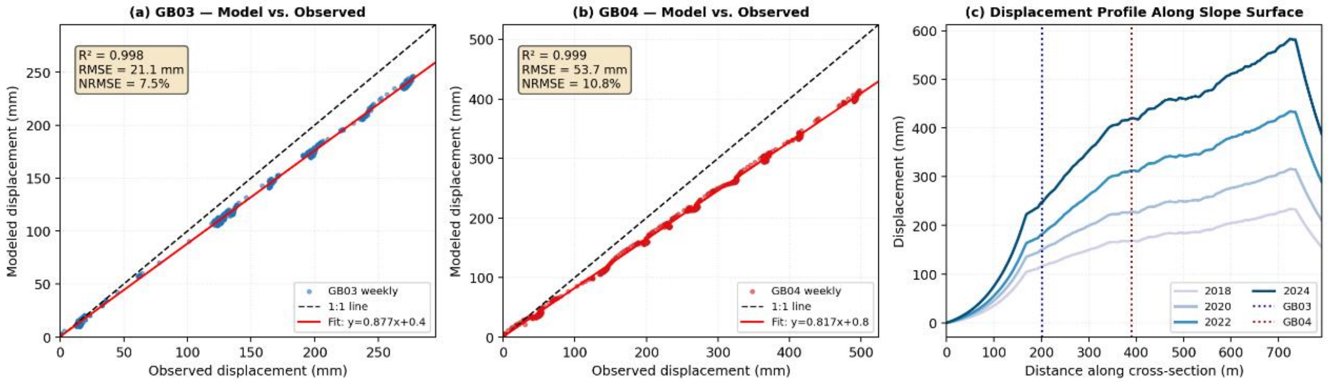

Figure 11: PyLith model validation and slope displacement characteristics.

6.2.4 Limitations and Future Perspectives

The PyLith-based finite element model developed in this study achieves an effective inversion from discrete monitoring points to a continuous displacement field, validating the applicability of GNSS-constrained fault slip methods in reservoir landslide simulations. Nevertheless, several limitations warrant further investigation. First, the simplification of constitutive relations: the current elastic model cannot account for plastic yielding or creep along the sliding surface, resulting in a 10–20% underestimation of seasonal accelerations; incorporating elastoplastic (e.g., Drucker-Prager (Klár et al., 2016)) or viscoelastic laws would refine these results. Second, the influence of dimensional reduction: the 2D plane-strain assumption neglects lateral constraints and 3D boundary effects, necessitating the transition to 3D mechanical modeling for enhanced fidelity. Third, the spatial resolution of boundary forcing: the extrapolation of the slip field from sparse GNSS points introduces localized uncertainties, which could be significantly mitigated by integrating areal displacement data, such as InSAR. In summary, this framework provides a robust quantitative tool for the dynamic risk assessment of reservoir landslides and offers a practical numerical analysis template for geohazard mitigation in the TGR area.

https://doi.org/10.5194/egusphere-2026-2913
Preprint. Discussion started: 6 August 2026

7 Conclusions

To address the challenges of mechanistic distortion and mode mixing in the decomposition of step-like landslide displacement sequences, this study developed an adaptive displacement decomposition framework embedded with physical constraints. Based on the empirical validation using long-term monitoring data from the TGR area, the primary conclusions are summarized as follows:

- Physics-informed parameter optimization significantly enhances the mechanistic interpretability of components. The CLF-SSA algorithm was successfully implemented to automate the selection of core VMD parameters. A pioneering joint fitness function, incorporating correlation penalties related to environmental drivers, ensures that the decomposition process is informed by physical laws. Results indicate that the reconstructed periodic components exhibit exceptional statistical significance with reservoir water levels (RWL), ensuring that the decomposition transcends purely mathematical fitting to achieve a mechanistic-oriented interpretation.
- Multidimensional reconstruction strategies effectively preserve the "step-like" features of non-stationary signals. A classification logic integrating center frequencies, multi-source environmental correlations, and seasonal energy distributions was established to achieve robust clustering into "trend, periodic, and stochastic" components. The model demonstrates sub-millimeter reconstruction precision (RMSE: 0.435 – 0.567 mm) with correlation coefficients exceeding 0.9999 across all stations. This high fidelity ensures that critical abrupt "step-jump" features are fully preserved, overcoming the loss of early-warning information inherent in conventional models due to over-smoothing.
- The component-based monitoring paradigm provides a novel scientific path for precision landslide early warning. Displacement decoupling under physical constraints yields a profound signal amplification effect, with the correlation gain of periodic responses reaching up to 4283.60%. This paradigm shift — transitioning from "unidimensional cumulative displacement" to "trend-periodic synergistic criteria" — effectively eliminates the masking effect of the dominant trend component. This transition significantly enhances the sensitivity of the system to environmental impulsive responses, thereby shortening warning lag times and providing a practical numerical foundation for intelligent and refined landslide risk management.

Code and data availability

The 10-year co-registered time-series dataset of key-station GNSS displacements, elevations, and hydro-meteorological driving factors (reservoir water levels and rainfall) used to validate the methodology is openly available and deposited in Zenodo repository at https://zenodo.org/records/21482916 (Liu et al., 2026). The source code, execution scripts, and the peer-review package for the physics-constrained adaptive displacement decomposition framework (CLF-SSA-VMD) developed in this study are publicly hosted on GitHub at https://github.com/liyix39/Physics-Constrained-VMD-Landslide-

Displacement-Decomposition (Li et al., 2026) and on Zenodo at https://zenodo.org/records/21483154. Both the dataset and the model code are distributed under the Creative Commons Attribution 4.0 International (CC BY 4.0) license.

Author contributions

YML developed the model code, designed the experiments, and performed the simulations. YXL contributed to the code development and engineering implementation. XF was responsible for data acquisition and project support. HC supervised the research, performed the manuscript review and editing, and prepared the landslide orthophotos. YML prepared the manuscript with contributions from all co-authors.

Competing interests

The contact author has declared that none of the authors has any competing interests.

Disclaimer

Publisher's note: Copernicus Publications remains neutral with regard to jurisdictional claims made in the text, published maps, institutional affiliations, or any other geographical representation in this paper. The authors bear the ultimate responsibility for providing appropriate place names. Views expressed in the text are those of the authors and do not necessarily reflect the views of the publisher.

Acknowledgements

The authors would like to express their sincere gratitude to Institute of Exploration Technology, CGS, for providing the long-term monitoring data and essential technical support that made this research possible. We are particularly grateful to the Yunyang geological hazard monitoring and early warning station in Chongqing for the use of its research infrastructure and field facilities in the TGR area, which served as the primary site for our data collection and empirical validation. Special thanks are also extended to our colleagues at the Institute for their invaluable field assistance and insightful discussions during the execution of this study.

Financial support

This work was supported by Project funded by National Natural Science Foundation of China (41804089), National Geological Safety Monitoring and Early Warning Network Operation and Maintenance of China (DD20251300206) and China Postdoctoral Science Foundation (2019M650782).

https://doi.org/10.5194/egusphere-2026-2913
Preprint. Discussion started: 6 August 2026

References

Aagaard, B., Knepley, M., and Williams, C.: PyLith v2.2.0, Zenodo [code], https://doi.org/10.5281/zenodo.165995, 2017.

Bjordal, J., Smith Jr., A. A., Cornec, H., and Storelvmo, T.: NorESM2–DIAM: a coupled model for investigating global and regional climate-economy interactions, Geosci. Model Dev., 19, 1337 – 1365, https://doi.org/10.5194/gmd-19-1337-2026, 2026.

Box, G. E. P., Jenkins, G. M., Reinsel, G. C., and Ljung, G. M.: Time series analysis: forecasting and control, John Wiley & Sons, 2015.

Bradley, K., Mallick, R., Andikagumi, H., et al.: Earthquake-triggered 2018 Palu Valley landslides enabled by wet rice cultivation, Nat. Geosci., 12, 935–939, https://doi.org/10.1038/s41561-019-0444-1, 2019.

Casagli, N., Intrieri, E., Tofani, V., Gigli, G., and Raspini, F.: Landslide detection, monitoring and prediction with remote-sensing techniques, Nat. Rev. Earth Environ., 4, 51–64, https://doi.org/10.1038/s43017-022-00373-x, 2023.

Chae, B. G., Park, H. J., Catani, F., Simoni, A., and Berti, M.: Landslide prediction, monitoring and early warning: a concise review of state-of-the-art, Geosci. J., 21, 1033–1070, https://doi.org/10.1007/s12303-017-0034-4, 2016.

Chen, H., Li, Y., and Liu, Y.: Research and analysis of the TCN-Multihead-Attention prediction model of landslide deformation in the Three Gorges Reservoir area, China, Front. Earth Sci., 13, 1587623, https://doi.org/10.3389/feart.2025.1587623, 2025.

Chen, J., Yang, Z., and Li, X.: Relationship between landslide probability and rainfall in Three Gorges Reservoir area, Chin. J. Rock Mech. Eng., 24, 3052–3056, https://doi.org/10.3321/j.issn:1000-6915.2005.17.008, 2005 (in Chinese with abstract in English).

Deng, M., Yi, Q., and Lu, Q.: Study on the deformation law and mechanism of chair-shaped soil landslide in Three Gorges Reservoir area, South-to-North Water Transf. Water Sci. Technol., 18, 135 – 143, https://doi.org/10.13476/j.cnki.nsbdqk.2020.0036, 2020 (in Chinese with abstract in English).

Dragomiretskiy, K. and Zosso, D.: Variational mode decomposition, IEEE Trans. Signal Process., 62, 531 – 544, https://doi.org/10.1109/TSP.2013.2288675, 2013.

Feng, Y., Tu, P., and Zeng, H.: A method for identifying critical displacement threshold of landslide step under combined effects of rainfall and reservoir water level, Chin. J. Rock Mech. Eng., 42, 2788 – 2805, https://doi.org/10.13722/j.cnki.jrme.2022.1311, 2023 (in Chinese with abstract in English).

Guo, F., Huang, X., Deng, M., Yi, Q., Zhang, P., Chen, J., and Chen, L.: Study on deformation mechanism and warning model of step-like landslide in Three Gorges Reservoir area, Acta Geod. Cartogr. Sin., 51, 2205 – 2215, https://doi.org/10.11947/j.AGCS.2022.20220296, 2022 (in Chinese with abstract in English).

Guo, Z., Chen, L., Gui, L., Du, J., Yin, K., and Do, H. M.: Landslide displacement prediction based on variational mode decomposition and WA-GWO-BP model, Landslides, 17, 567–583, https://doi.org/10.1007/s10346-019-01314-4, 2020.

https://doi.org/10.5194/egusphere-2026-2913
Preprint. Discussion started: 6 August 2026

Guo, Z., Yin, K., Liu, Q., Huang, F., Gui, L., and Zhang, G.: Rainfall Warning of Creeping Landslide in Yunyang County of Three Gorges Reservoir Region Based on Displacement Ratio Model, Earth Sci., 45, 672 – 684, https://doi.org/10.3799/dqkx.2019.005, 2020 (in Chinese with abstract in English).

Intrieri, E., Gigli, G., Mugnai, F., Fanti, R., and Casagli, N.: Design and implementation of a landslide early warning system, Eng. Geol., 147, 124–136, https://doi.org/10.1016/j.enggeo.2012.07.017, 2012.

Jiang, Y., Zheng, L., Xu, Q., and Lu, Z.: Deformation mechanism-assisted deep learning architecture for predicting step-like displacement of reservoir landslide, Int. J. Appl. Earth Obs. Geoinf., 133, 104121, https://doi.org/10.1016/j.jag.2024.104121, 2024.

Jiang, Y., Zheng, L., Xu, Q., Tang, M., and Zhu, X.: Step-like displacement prediction of landslides guided by deformation mechanism, Acta Geod. Cartogr. Sin., 53, 1128−1139, https://doi.org/10.11947/j.AGCS.2024.20230463, 2024 (in Chinese with abstract in English).

Jiang, Y., Wang, W., and Zou, L.: Dynamic prediction model of landslide displacement based on particle swarm variational mode decomposition, nonlinear autoregressive neural network and gated cycle unit, Rock Soil Mech., 43, 601–612, 2022 (in Chinese with abstract in English).

Klár, G., Gast, T., Pradhana, A., Fu, C., Schroeder, C., Jiang, C., and Teran, J.: Drucker-Prager elastoplasticity for sand animation, ACM Trans. Graph., 35, 1–12, https://doi.org/10.1145/2897824.2925906, 2016.

Li, W. N.: Study on dynamic deformation response and permeability of hydrodynamic pressure-type accumulation landslides in the Three Gorges Reservoir area, PhD thesis, China University of Geosciences, Wuhan, China, 2023 (in Chinese).

Li, Y., and Liu, Y.: Physics-constrained VMD landslide displacement decomposition review package, GitHub [code], https://github.com/liyix39/Physics-Constrained-VMD-Landslide-Displacement-Decomposition, 2026.

Liu, Y., Chen H. and Li, Y.: A physics-constrained adaptive decomposition model for displacement sequences of step-like landslide, Zenodo [code], https://zenodo.org/records/21483154, 2026.

Liu, Y., Li, Y., Feng, X., and Chen, H.: GNSS displacements and environmental driving factors dataset of three monitoring stations at the Yutang landslide (2015–2025), Zenodo [data set], https://zenodo.org/records/21482916, 2026.

Lu, S., Yi, Q., Yi, W., Zhang, G., and He, X.: Study on dynamic deformation mechanism of landslide in drawdown of reservoir water level — take Baishuihe Landslide in Three Gorges Reservoir area for example, J. Eng. Geol., 22, 869–875, https://doi.org/10.13544/j.cnki.jeg.2014.05.15, 2014 (in Chinese with abstract in English).

Meng, Y., Qin, Y., Cai, Z., Tian, B., Yuan, C., Zhang, X., and Zuo, Q.: Dynamic forecast model for landslide displacement with step-like deformation by applying GRU with EMD and error correction, Bull. Eng. Geol. Environ., 82, 211, https://doi.org/10.1007/s10064-023-03247-8, 2023.

Pardeshi, S. D., Autade, S. E., and Pardeshi, S. S.: Landslide hazard assessment: Recent trends and techniques, SpringerPlus, 2, 523, https://doi.org/10.1186/2193-1801-2-523, 2013.

Pecoraro, G., Calvello, M., and Piciullo, L.: Monitoring strategies for local landslide early warning systems, Landslides, 16, 213–231, https://doi.org/10.1007/s10346-018-1068-z, 2019.

https://doi.org/10.5194/egusphere-2026-2913
Preprint. Discussion started: 6 August 2026

Qu, J. K., Zhu, Q. Y., Qi, S. C., and Zhou, J.: Instability mechanism of reservoir landslides under combined effects of water level fluctuations and rainfall, Eng. Geol., 352, 108092, https://doi.org/10.1016/j.enggeo.2025.108092, 2025.

Raj, S. and Ray, K. C.: Application of variational mode decomposition and ABC optimized DAG-SVM in arrhythmia analysis, 2017 7th International Symposium on Embedded Computing and System Design (ISED), Durgapur, India, 1–5, https://doi.org/10.1109/ISED.2017.8303935, 2017.

Ren, S., Ghazali, K. H., Ji, Y., and Khan, S. U.: Landslide Displacement Prediction Model Based on Optimal Decomposition and Deep Attention Mechanism, IEEE Access, 13, 51573–51588, https://doi.org/10.1109/ACCESS.2025.3551730, 2025.

Segoni, S., Piciullo, L., and Gariano, S. L.: Preface: Landslide early warning systems: monitoring systems, rainfall thresholds, warning models, performance evaluation and risk perception, Nat. Hazards Earth Syst. Sci., 18, 3179–3186, https://doi.org/10.5194/nhess-18-3179-2018, 2018.

Segoni, S., Piciullo, L., and Gariano, S. L.: A review of the recent literature on rainfall thresholds for landslide occurrence, Landslides, 15, 1483–1501, https://doi.org/10.1007/s10346-018-0966-4, 2018.

Song, K., Yang, H., Liang, D., Chen, L., and Jaboyedoff, M.: Step-like displacement prediction and failure mechanism analysis of slow-moving reservoir landslide, J. Hydrol., 628, 130588, https://doi.org/10.1016/j.jhydrol.2023.13058, 2024.

Sun, X. and Zhao, J.: Analysis on the runoff regulation of Three Gorges Reservoir, J. Water Resour. Res., 8, 1–10, https://doi.org/10.12677/JWRR.2019.86063, 2019 (in Chinese with abstract in English).

Wang, Z. H., Nie, W., and Xu, H. H.: Prediction of landslide displacement based on EEMD-prophet-LSTM, J. Univ. Chin. Acad. Sci., 40, 514–522, https://doi.org/10.7523/j.ucas.2022.002, 2023 (in Chinese with abstract in English).

Wen, T., Tang, H., Wang, Y., Lin, C., and Xiong, C.: Landslide displacement prediction using the GA-LSSVM model and time series analysis: a case study of Three Gorges Reservoir, China, Nat. Hazards Earth Syst. Sci., 17, 2181–2198, https://doi.org/10.5194/nhess-17-2181-2017, 2017.

Wu, H., Huang, P., Tan, W., Qi, Y., Xu, W., and Chen, Y.: A new early warning method for landslide critical sliding tangent angle based on modified Nishihara model, Eng. Geol., 356, 108283, https://doi.org/10.1016/j.enggeo.2025.108283, 2025.

Xiang, X., Wen, H., Xiao, J., Wang, X., Yin, H., and Huang, J.: Analyzing failure mechanisms and predicting step-like displacement: Rainfall and RWL dynamics in lock-unlock landslides, Geosci. Front., 16, 1–19, https://doi.org/10.1016/j.gsf.2024.101959, 2025.

Yin, Y.: Human-cutting slope structure and failure pattern at the Three Gorges Reservoir, J. Eng. Geol., 13, 145–155, 2005 (in Chinese with abstract in English).

Yin, Y.: Research on Major Geological Hazards and Prevention at New Relocation Sites for Migrants in the Three Gorges Reservoir Area of the Yangtze River, The Geological Publishing House, Beijing, 2004 (in Chinese).